Studia Geotechnica et Mechanica, Vol. XXXVI, No. 1, 2014 DOI: 10.2478/sgem-2014-0004

EDGE DETECTION ON IMAGES OF PSEUDOIMPEDANCE SECTION SUPPORTED BY CONTEXT AND ADAPTIVE TRANSFORMATION MODEL IMAGES

EWA KAWALEC-LATAŁA

AGH University of Science and Technology,
Faculty of Geology, Geophysics and Environment Protection, Kraków, Poland.

Abstract: Most of underground hydrocarbon storage are located in depleted natural gas reservoirs. Seismic survey is the most economical source of detailed subsurface information. The inversion of seismic section for obtaining pseudoacoustic impedance section gives the possibility to extract detailed subsurface information. The seismic wavelet parameters and noise briefly influence the resolution. Low signal parameters, especially long signal duration time and the presence of noise decrease pseudoimpedance resolution. Drawing out from measurement or modelled seismic data approximation of distribution of acoustic pseuoimpedance leads us to visualisation and images useful to stratum homogeneity identification goal. In this paper, the improvement of geologic section image resolution by use of minimum entropy deconvolution method before inversion is applied. The author proposes context and adaptive transformation of images and edge detection methods as a way to increase the effectiveness of correct interpretation of simulated images. In the paper, the edge detection algorithms using Sobel, Prewitt, Robert, Canny operators as well as Laplacian of Gaussian method are emphasised. Wiener filtering of image transformation improving rock section structure interpretation pseudoimpedance matrix on proper acoustic pseudoimpedance value, corresponding to selected geologic stratum. The goal of the study is to develop applications of image transformation tools to inhomogeneity detection in salt deposits.

Key words: *underground storage, acoustic impedance, data analysis and visualisation, edge detection algorithms, rock salt, inhomogeneity detection*

1. INTRODUCTION

Rock mass containing salt deposits display high seismologic inhomogeneity. Correct detection of inhomogeneity of horizontal or semi-horizontal stratum of rocky salt deposits are crucial in preparation of reservoirs.

The acoustic impedance changes with lithologic and facial changes in subsurface. The inversion of seismic section for obtaining pseudoacoustic impedance section gives the possibility to bind very closely with geological data and gives the possibility to extract additional information from seismic data. The inversion process effectively transforms seismic information into the geological domain. The quality and quantity of interpretation of the final results increase with the frequency bandwidth of seismic data and dominant frequency increase. The basic inversion concept is simple; a reversal of the procedure long used to compute synthetic seismograms from sonic logs is the first idea. Many different approaches are applied to achieve the goal [12]. In practice the reverse process is difficult, since it requires inversion of a low grade, the seismic trace, into the higher-grade sonic log signal. A reflection coefficient time series should be represented by a single spike. The synthetic seismic trace is given by convolution reflection coefficients series and seismic wavelet

$$x(t) = r(t) * w(t) \tag{1}$$

where

$r(t)$ – reflection coefficient series,
$w(t)$ – seismic wavelet,
$x(t)$ – synthetic seismic trace.

The synthetic seismic trace with noise is given by

$$x(t) = r(t) * w(t) + n(t) \tag{2}$$

where

$r(t)$ – reflection coefficient series,
$w(t)$ – seismic wavelet,
$x(t)$ – synthetic seismic trace,
$n(t)$ – random noise.

The real data are briefly distorted especially by transmission losses, random noise, phenomena associ-

ated with the recorded seismic signal and band limited wavelet. The main step in the inversion process is adequate processing seismic data before inversion. Modern seismic field data can be processed to eliminate much of the distortion, and can be compensated in part wave propagation phenomena and density, to yield an approximation to reflection coefficients. First, seismic traces are converted into pseudoreflection coefficient time series, then into acoustic impedance by the inversion of the time series. A reflection coefficient time series should be represented by a single spike. An important procedure to repair damage to the spectrum (caused by transmission trough the earth and the recording instruments) is deconvolution. Ideally, an acoustic impedance interface should be represented by a single spike on the seismic section.

Pseudoacoustic impedance section obtained by inversion of seismic section facilitates the interpretation, but the seismic wavelet parameters and noise briefly influence the resolution. Low dominant frequency and especially long signal duration time and the presence of noise decrease pseudoimpedance resolution [9]. One of the methods to improve the resolution thorough processing before the inversion process is especially the deconvolution. The other is the image processing after the inversion process.

Image processing and edge detection presented in the paper are based on synthetic pseudoimpedance acoustic section of seismic-geology model as standard detection of salt deposits in our country.

The edge detection of analysed images uses Sobel operator, Prewitt operator, Robert operator, Canny operator as well as Laplacian of Gaussian method, Wiener filtering and by slicing 3-D acoustic pseudoimpedance matrix into proper acoustic pseudoimpedance value, corresponding to selected geologic stratum.

2. SEISMIC MODELLING OF PSEUDOIMPEDANCE ACOUSTIC SECTIONS

The synthetic pseudoimpedance acoustic sections presented in this paper are generated for the simplified data from LGOM areas obtained by inversion method based on recursive relation. The rock salt on synthetic pseudoimpedance acoustic sections is observed in

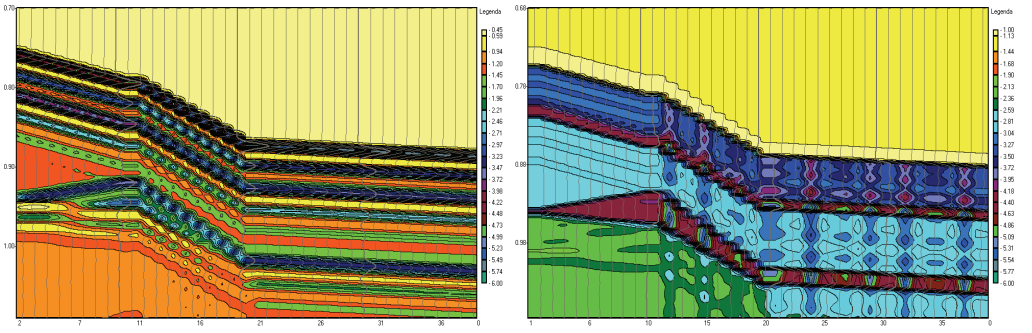

a) b)

Fig. 1. Synthetic pseudoimpedance acoustic section.
The parameters of signal applied to construction of synthetic seismogram are: f_0 – dominant frequency 40 Hz, $f_0/\beta = 2$

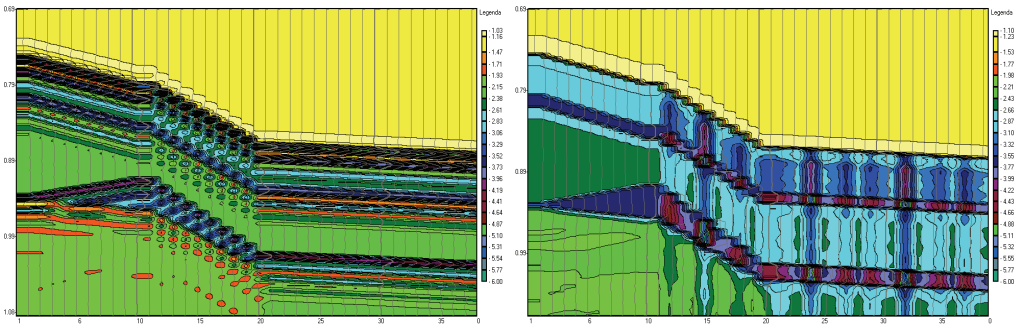

a) b)

Fig. 2. Synthetic pseudoimpedance acoustic section.
The parameters of signal applied to construction of synthetic seismogram are: f_0 – dominant frequency 40 Hz, $f_0/\beta = 2$

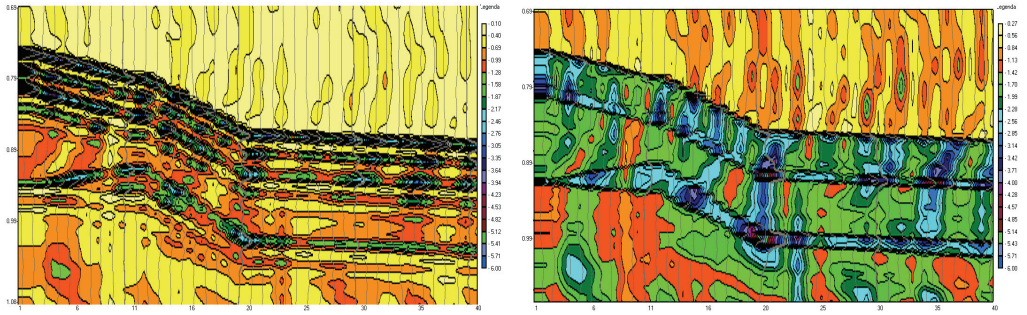

a) b)

Fig. 3. Synthetic pseudoimpedance acoustic section.
The parameters of signal applied to construction of synthetic seismogram are: f_0 – dominant frequency 40 Hz, $f_0/\beta = 2$, noise 30%

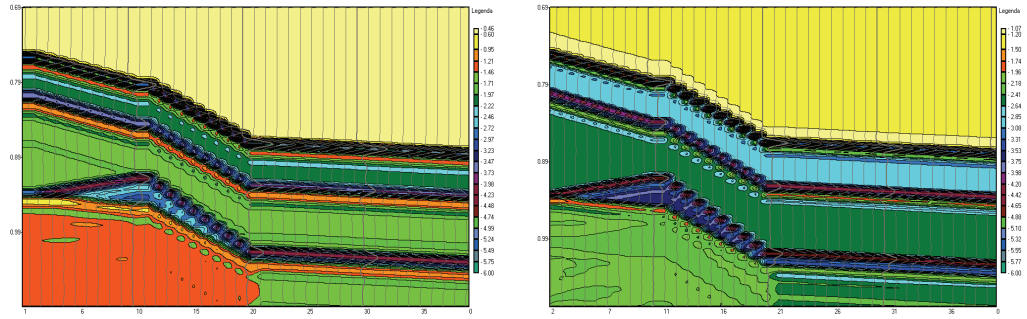

a) b)

Fig. 4. Synthetic pseudoimpedance acoustic section.
The parameters of signal applied to construction of synthetic seismogram are: f_0 – dominant frequency 40 Hz, 60 Hz, $f_0/\beta = 1$

time limit between 0.70–1.00 s (1000 m and 1600 m, respectively, on the geological model).

The synthetic pseudoimpedance acoustic section presented in Figs. 1–3 are generated for long signal duration time $f_0/\beta = 2$ (f_0 – dominant frequency, β – dumping factor), for dominant frequency $f_0 = 40$ Hz, in Fig. 1, for dominant frequency $f_0 = 60$ Hz in Fig. 2, for dominant frequency $f_0 = 60$ Hz and random noise added to synthetic seismic section in Fig. 3. The synthetic pseudoimpedance acoustic sections generated without deconvolution are presented in Figs. 1a, 2a, 3a and with deconvolution minimum entropy MED applied before process inversion are presented in Figs. 1b, 2b, 3b.

The synthetic pseudoimpedance acoustic sections generated for short signal duration time $f_0/\beta = 1$ are presented in Fig. 4, for dominant frequency $f_0 = 40$ Hz (Fig. 4a) and $f_0 = 60$ Hz (Fig. 4b).

From the comparison of the resolution of pseudoimpedance acoustic sections, Figs. 1–4, the effect of deconvolution minimum entropy (MED) can be observed. The effect of long time signal duration is compensated by the deconvolution minimum entropy MED which is done before inversion process. That enhances the precision of interpretation, but the effect of compensation is not so visible in the presence of noise.

In the paper, the minimum entropy deconvolution (MED) before inversion synthetic data generated by INVERS system is applied. MED technique was proposed by Wiggins [13], it performs maximisation of an entropy norm, so called the Varimax norm. In the original approach, the term "minimum entropy" is a synonym of "maximum order". Minimum entropy deconvolution MED norm seeks the smallest number of large spikes that are consistent with the data mainly of isolated spikes Dirac $\delta(t)$. The solution consists of reasonable feature of reflectivity. That means that in practice a high reflection coefficient influences much more the solution.

Internal structure of the salt deposit displays several lithological types of rock salt (pure coarse-crystalline salt, anhydrite salt, salt intercalated with anhydrite). Rock mass containing salt deposits displays high seismologic inhomogeneity. Due to considerable contrast of elastic properties of different kinds of salts and unlike neighbouring layers the high reflection coefficients are observed within the Zechstein rocks. That is consistent with theoretical features of minimum entropy deconvolution (MED).

3. COMPUTER AID IN GEOLOGIC FEATURE IDENTIFICATION

From aggregated data, in many cases, there is constructed a set of data that establish knowledge base to built images of properties of the modelled geologic morphology. Visualisation of data sets takes the form of some images as well as colours or grey.

The most frequently used geometric conversions of image with computer aided technique are context and spectrum transformation as well as different forms of a morphology mapping [1], [2]. Context transformation is based on alteration of image elements depending on their own content and content of circumambient elements. It requires a lot of calculations and recalculations on the basis of surrounding image elements to achieve value of transformed image element. Those operations are defined by convolution function. Convolution provides a way of "multiplying together" two arrays of numbers, generally of different sizes, but of the same dimensionality, to produce a third array of the same dimensionality. This can be used in image processing to implement operators whose output pixel values are simple linear combinations of certain input pixel values. In an image context processing, one of the input arrays (I) is normally just a greyscale image. The second array (K) is usually much smaller, and is also two-dimensional (although it may be just a single pixel thick), and is known as the kernel. Mathematically we can write the convolution as

$$O(i,j) = \sum_{k=1}^{m}\sum_{l=1}^{n} I(i+k-1, j+L-1)K(k,l) \qquad (3)$$

where i runs from 1 to $M - m + 1$ and j runs from 1 to $N - n + 1$, M, N are the sizes of arrays (I), m, n are the size of array (K).

The median and mean filtering methods will reduce the amount of noise contained in a signal, but will do nothing towards restoring a distorted image. It is a low-pass filtering method based on the assumption that each pixel is more or less like the ones around it. As a result, fine details may be lost, but a better feel for the entire image may be gained [14]. An example pictures of INVERS system model A42S30 – with ill-posed parameters as: low main frequency $f = 40$ [Hz], dumping factor $\beta = 20$, noise $s = 30\%$ are presented as mash visualisation of original matrix and after cutting off percentiles (1.99), and mash visualisation after median filtering.

An edge in an image is a sharp variation of the intensity function. In greyscale images this applies to the intensity or brightness of pixels. In colour images it can also refer to sharp variations of colour. An edge is distinguished from noise by possessing a long range structure. The properties of edges include gradient and orientation.

Edge detection is a terminology in image processing and computer vision, particularly in the areas of feature detection and feature extraction, to refer to algorithms which aim at identifying points in a digital image at which the image feature changes sharply or more formally has discontinuities. The edge detection methods [14] that have been published mainly differ in the types of smoothing filters that are applied and the way the measures of edge strength are computed. As many edge detection methods rely on the computation of image gradients, they also differ in the types of filters used for computing gradient estimates in the x- and y-directions.

Canny algorithm edge detection method is considering the mathematical problem of deriving an optimal smoothing filter given the criteria of detection, localisation and minimising multiple responses to a single edge. Canny showed that the optimal filter given these assumptions is a sum of four exponential terms. He also showed that this filter could be well approximated by first-order derivatives of Gaussians. Canny also introduced the notion of non-maximum suppres-

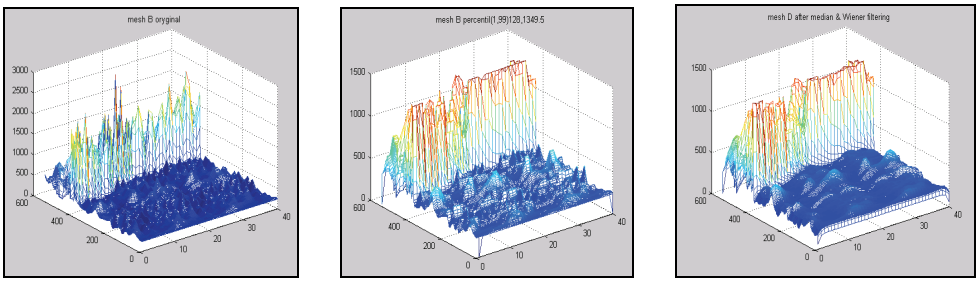

a) b) c)

Fig. 5. The sample of INVERT image model A42S30 as mash visualisation of:
(a) original matrix and (b) after cutting off percentiles (1.99), (c) mash visualisation after median filtering and Wiener's filtering

sion, which means that given the presmoothing filters, edge points are defined as points where the gradient magnitude assumes a local maximum in the gradient direction. The Canny–Deriche detector was derived from similar mathematical criteria as the Canny edge detector, although starting from a discrete viewpoint and then leading to a set of recursive filters for image smoothing instead of exponential filters or Gaussian filters.

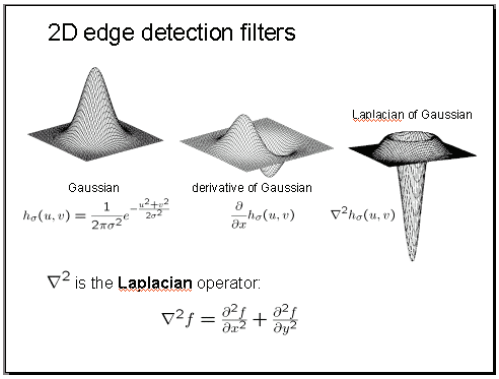

Fig. 6. Picture of two-dimensional edge detection filters

For estimating image gradients from the input image or a smoothed version of it, different gradient operators can be applied. The simplest approach is to use central differences

$$\begin{aligned} L_x(x, y) &= -1/2 * L(x-1, y) \\ &+ 0 * L(x, y) + 1/2 * L(x+1, y), \\ L_y(x, y) &= -1/2 * L(x, y-1) \\ &+ 0 * L(x, y) + 1/2 * L(x, y+1) \end{aligned} \tag{4}$$

corresponding to the application of the following filter masks to the image data

$$L_x = [-1/2 \;\; 0 \;\; 1/2] * L$$

and $$L_y = [+1/2 \;\; 0 \;\; -1/2]^T * L.$$

The well-known and earlier Sobel operator is based on the following filters

$$\begin{aligned} L_x &= \begin{bmatrix} -1 & 0 & +1 \\ -2 & 0 & +2 \\ -1 & 0 & +1 \end{bmatrix} * L, \\ L_y &= \begin{bmatrix} +1 & +2 & +1 \\ 0 & 0 & 0 \\ -1 & -2 & -1 \end{bmatrix} * L. \end{aligned} \tag{5}$$

Given such estimates of first-order derivatives, the gradient magnitude is then computed as

$$\left|\nabla L\right| = \sqrt{L_x^2 + L_y^2}\,, \tag{6}$$

while the gradient orientation can be estimated as

$$\theta = a\tan 2(L_y, L_y)\,. \tag{7}$$

The Kayyali operator extracted from Sobel operator based on two directions, which has direction (South East North West) known as Kayyali SENW and another direction (North East South West) known as Kayyali NESW is shown below

$$\begin{aligned} Kayyali\_SENW &= \begin{bmatrix} +6 & 0 & -6 \\ 0 & 0 & 0 \\ -6 & 0 & +6 \end{bmatrix}, \\ Kayyali\_SENW &= \begin{bmatrix} -6 & 0 & +6 \\ 0 & 0 & 0 \\ +6 & 0 & -6 \end{bmatrix}. \end{aligned} \tag{6}$$

Other first-order difference operators for estimating image gradient have been proposed in the Prewitt operator and Roberts cross.

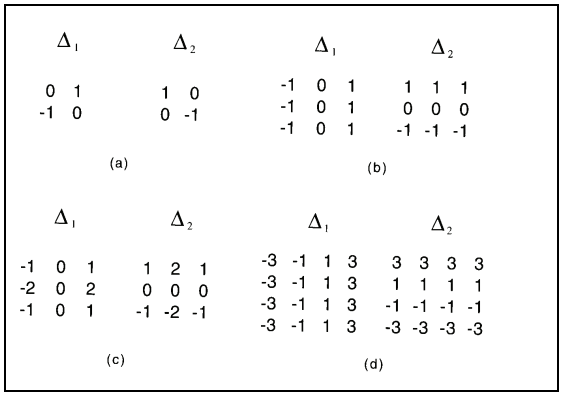

Fig. 7. Gradient operators used in edge detection algorithms: (a) Roberts' cross operator, (b) 3 × 3 Prewitt operator, (c) Sobel operator, (d) 4 × 4 Prewitt operator

A recent development in edge detection techniques called Phase Congruency Based Edge Detection takes a frequency domain approach to finding edge locations. Phase congruency (also known as phase coherence) methods attempt to find locations in an image where all sinusoids in the frequency domain are in phase. These locations will generally correspond to the location of a perceived edge, regardless of whether the edge is represented by a large change in intensity in the spatial domain. A key benefit of this technique is that it responds strongly to Mach bands, and avoids false positives typically found around roof edges.

4. EXEMPLIFICATION OF EDGE DETECTION IN GEOLOGIC INTERPRETATION OF ACOUSTIC PSEUDOIMPEDANCE IMAGES OF ROCKY SURROUNDINGS

Image processing tools applied in interpretation of acoustic pseudoimpedance picture are considered as a subject of increased effectiveness of correct interpretation of images simulated by INVERS system [5]. The sample results, obtained from the calculation on model A42S30 considered in the paper (Fig. 3), are gathered in Fig. 8.

The original matrix of acoustic pseudoimpedance up to now is pictured as colourful image. MATLAB function was used to form a greyscale image, so original matrix was recalculated to limited range of value (0–255) corresponding to greyscale. After the normalisation process, acoustic pseudoimpedance matrix was filtered by edge detecting algorithms, described before. Sample results are presented in Fig. 9.

Reading ability of the above images and proper geological interpretation are doubtful, so next step of investigation is an idea to detect edges of images transformed to logic matrix (grey images are changed to black and white pictures). Edge detection process consists of threshold selection for binary conversion, grain filtration, reintegration and dilatation of proc-

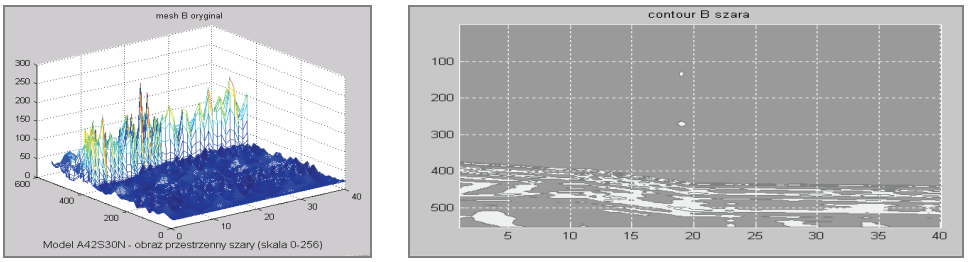

a) b)

Fig. 8. Picture of original matrix of model A42S30, normalised to grey scale (0–255) as (a) meshes and (b) contour grey image

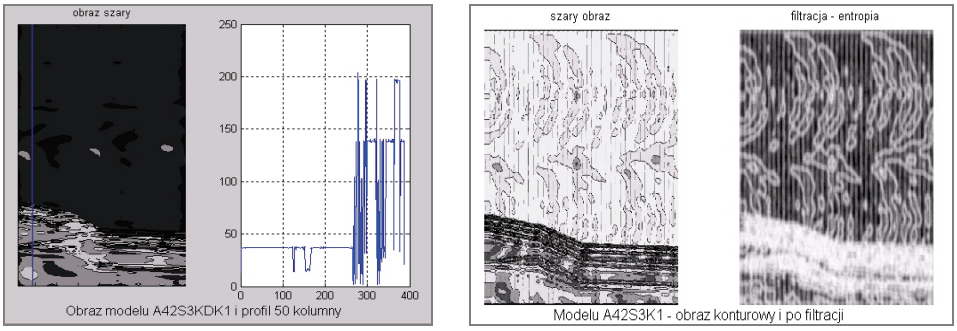

a) b) c) d)

Fig. 9. Greyscale image of A42S30 geologic morphology model (a), with profile chart (for market section on image) (b), contour image of A42S30 geologic morphology model (c), and its picture after smoothing and entropy filtration (d)

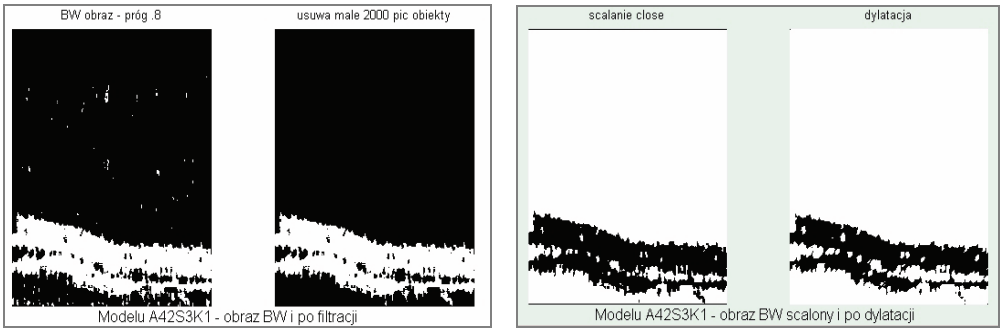

Fig. 10. Sample of images picturing conversion process to BW form (binarization), grain filtration, reintegration and dilatation of processed geologic section matrix

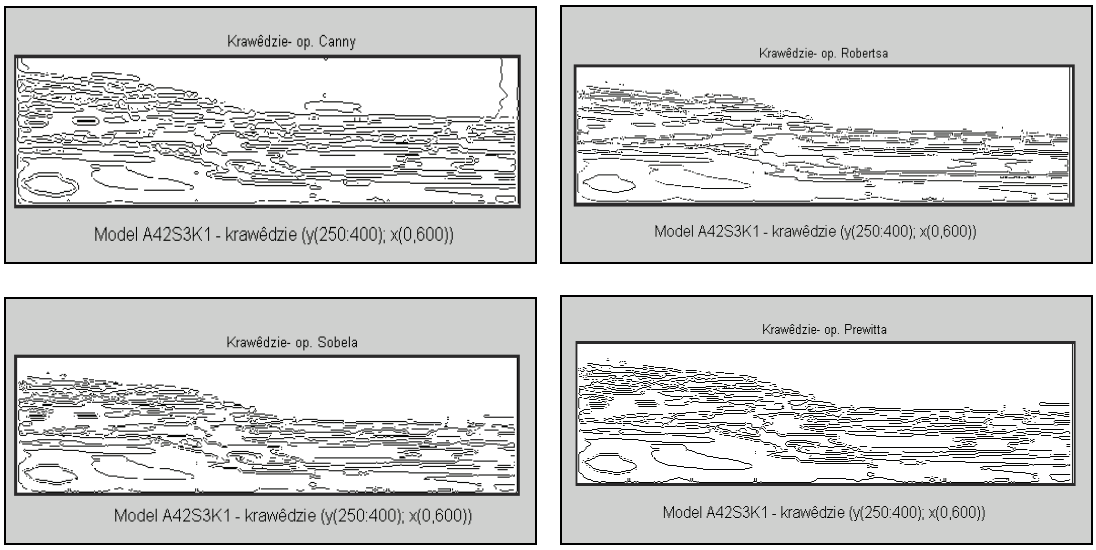

Fig. 11. Original acoustic pseudoimpedance matrix of model A42S30 after process edge detection with: (a) Canny, (b) Robert, (c) Sobel and (d) Prewitt algorithms accordingly

essed matrix [3], [10]. The process of conversion is pictured in Fig. 10.

Reading ability of those images and their proper geological interpretation is a little more accurate compared to results of edge detection with Prewitt/ Canny/Sobel/Roberts operator, illustrated in Fig. 11, but still not satisfactory.

The model A42S30 considered in the paper is intentionally disturbed by noise to simulate real condition of acoustic measurement. Keeping in memory, that original image and its matrix belong to difficult objects, any progress in readability and proper geologic interpretation should be taken.

An easy interpretation and detection of interesting stratum (for example, layer of rocky salt or anhydrite) is still doubtful. The concept, introduced in [6], to slice mash charts of acoustic pseudoimpedance matrix value on chosen level, proper for interesting stratum, is still up-to-date. The contour charts were filled by colour, depending on acoustic pseudoimpedance selected value, presented in [5], are comparable with results presented in Fig. 10.

5. SUMMARY OF RESULTS AND CONCLUSIONS

The best hydrocarbon reservoirs are constructed in salt deposits. First, the detection and identification of salt stratum inhomogenity are required. This can be done on the basis of seismic surface measurement. The seismic section in pseudoacoustic impedance version facilitates the interpretation. Due to limited frequency bandwidth of seismic data and the presence of noise, the inversion procedure is not unambiguous. The results are validated as an image, whose quality can be improved by deconvolution process. In the paper, serviceability of minimum entropy deconvolution (MED) method to correct resolution of seismic section images is presented. In the presence of noise the (MED) method gives no satisfying improvements.

Image processing and edge detection presented in the paper are based on synthetic pseudoimpedance acoustic section of simple seismogeological model as standard salt deposit from LGOM area. The model A42S30 and its clones, generated for the geological configuration of salt deposit with anhydrite intercalation were materials studied for parameter selection of image processing. Those difficult conditions, especially low signal parameters and relatively high noise level of 30% were assumed in modelling. Conclusions drawn from the investigation suggest prudence in optimism, because context filtering even complying with adaptive filters is sensitive to context extent. The best results of Wiener filtering can be obtained for the noise parameters determined, which is in real measurement difficult.

In the present paper, edges of analysed images were detected using the Sobel operator, Prewitt operator as well as Laplacian of Gaussian method and by slicing a 3-D acoustic pseudoimpedance matrix into proper acoustic pseudoimpedance value, corresponding to selected geologic stratum.

The Sobel operator is based on convoluting the image with a small, separable, and integer valued filter in horizontal and vertical direction so the gra-

dient approximation is relative crude. Its advantage is relatively inexpensiveness in terms of computations.

The Prewitt method is called edge template matching, because a set of edge templates is matched to the image, each representing an edge in a certain orientation. The edge magnitude and orientation of a pixel are determined by one but of eight templates that matches best the local area of the pixel.

The result for the edge magnitude image is very similar with both (Sobel and Prewitt) methods, provided the same convoluting kernel is used.

The Laplacian, as isotropic measure on plane of the 2nd spatial derivative of an image, highlights regions of rapid intensity change and therefore is used in our analysis for edge detection. The Laplacian is applied to investigate image that has first been smoothed with Wiener smoothing filter in order to reduce its sensitivity to noise.

In the paper, an idea to detect edges of images transformed to logic matrix (grey images are changed to black and white pictures) is presented. Edge detection process consists of threshold selection for binary conversion, grain filtration, reintegration and dilatation of processed matrix.

The images of selected stratum (anhydrite) are presented as contour charts filled with colour depending on the value of acoustic pseudoimpedance (set of a few values for given range). The sliding process of mash chart of acoustic pseudoimpedance matrix value on chosen level, proper for interesting stratum has most interesting results, but still not enough to be satisfactory.

ACKNOWLEDGEMENT

The work was supported by Geophysics Dept. AGH UST project (no. 11.11.140.769).

REFERENCES

[1] BOYLE R., SONKA M., HLAVAC V., *Image Processing, Analysis, and Machine Vision*, First Edition, University Press, Cambridge, 1993.

[2] BROADHEAD M.K., PFLUG L.A., *Deconvolution for transient classification using fourth order statistics*, Naval Research Laboratory, Acoustics Division, Stennis Space Center, MS 39529-5009, USA.

[3] CANNY J., *A Computational Approach To Edge Detection*, IEEE Trans. Pattern Analysis and Machine Intelligence, 1986, 8, 679–714.

[4] DERICHE R., *Using Canny's criteria to derive an optimal edge detector recursively implemented*, Int. J. Computer Vision, April 1987, Vol. 1, 167–187.

[5] FIGIEL W., KAWALEC-LATAŁA E., *Context and adaptive transformation applied to interpretation of acoustic pseudoimpedance images of rocky surroundings*, Gospodarka Surowcami Mineralnymi, 2009, t. 25, z. 3, 273–288.

[6] FIGIEL W., KAWALEC-LATAŁA E., *Zastosowanie analizy i przetwarzania obrazów do interpretacji syntetycznych sekcji pseudoimpedancji akustycznej*, Gospodarka Surowcami Mineralnymi, 2008, t. 24, z. 2/3, 371–385.

[7] GONZALES R.C., WINTZ P., *Digital Image Processing*, Second Edition, Addison-Wesley Publishing Co., Massachusets, 1987.

[8] HUNT B.R., *The Application of Constrained Least Squares Estimation to Image Restoration by Digital Computer*, IEEE Transactions on Computers, September 1973, Vol, C-22, No. 9.

[9] KAWALEC-LATAŁA E., *The influence of seismic wavelet on the resolution of pseudo impedance section for construction of underground storage*, Gospodarka Surowcami Mineralnymi, 2008, t. 24, z. 2/3, 387–397.

[10] LINDEBERG T., *Edge detection and ridge detection with automatic scale selection*, International Journal of Computer Vision, 1998, 30, 2, 117–154.

[11] PITAS J.I., *Digital Image Processing Algorithms*, Prentice Hall International (UK), Ltd., Cambridge, 1993.

[12] VEEKEN P.C.H., DA SILVA M., *Seismic inversion and some of their constrains*, First Break, 22 (6), 47–70.

[13] WIGGINS R.A., *Minimum Entropy Deconvolution*, Geoexploration, 1978, Vol. 16, 21–35.

[14] ZIOU D., TABBONE S., *Edge Detection Techniques An Overview*, International Journal of Pattern Recognition and Image Analysis, 1998, 8(4), 537–559.